

This is the accepted manuscript of the article, which has been published in Bowes Rickman, Catherine et al (eds) Retinal Degenerative Diseases: Mechanisms and Experimental Therapy. Cham: Springer. Advances in Experimental Medicine and Biology vol 1185. ISBN: 978-3-030-27378-1. ISSN: 2214-8019. [https://doi.org/10.1007/978-3-030-27378-1\\_86](https://doi.org/10.1007/978-3-030-27378-1_86)

## **Chapter XX**

# **Analysis of ATP-induced Ca<sup>2+</sup> Responses at Single Cell Level in Retinal Pigment Epithelium Monolayers**

Sorvari J<sup>1</sup>, Viheriälä T<sup>1</sup>, Ilmarinen T<sup>1</sup>, Ihalainen TO<sup>1</sup>, Nymark S<sup>1</sup>

### Affiliations

<sup>1</sup> Tampere University, Faculty of Medicine and Health Technology, BioMediTech Institute, Tampere, Finland

Corresponding Author:

Soile Nymark, [soile.nymark@tut.fi](mailto:soile.nymark@tut.fi)

## **Abstract**

Calcium is one of the most important second messengers in cells and thus involved in a variety of physiological processes. In retinal pigment epithelium (RPE),  $\text{Ca}^{2+}$  and its ATP-dependent signaling pathways play important roles in the retina maintenance functions. Changes in intracellular  $\text{Ca}^{2+}$  concentration can be measured from living cells by  $\text{Ca}^{2+}$  imaging. Combining these measurements with quantitative analysis of  $\text{Ca}^{2+}$  response properties enables studies of signaling pathways affecting RPE functions. However, robust tools for response analysis from large cell populations are lacking. We developed MATLAB-based analysis tools for single cell level  $\text{Ca}^{2+}$  response data recorded from large fields of intact RPE monolayers. The analysis revealed significant heterogeneity in ATP-induced  $\text{Ca}^{2+}$  responses inside cell populations regarding magnitude and response kinetics. Further analysis including response grouping and parameter correlations allowed us to characterize the populations at the level of single cells.

## **XX.1 Introduction**

Retinal pigment epithelium (RPE) resides between retina and choroid in the back of the eye and performs an array of functions vital for retinal welfare (Strauss, 2005). Several of these functions are regulated by changes in intracellular calcium ( $\text{Ca}^{2+}$ ) concentration ( $[\text{Ca}^{2+}]_i$ ) that can be experimentally measured by  $\text{Ca}^{2+}$  imaging using  $\text{Ca}^{2+}$  sensitive fluorescent dyes or fusion proteins. One activator of  $\text{Ca}^{2+}$  signaling in RPE is adenosine triphosphate (ATP): Light-induced increase in ATP near retinal photoreceptors and RPE apical membrane causes increase in  $[\text{Ca}^{2+}]_i$  via purinergic receptors and intracellular  $\text{Ca}^{2+}$  stores, and affects RPE transport processes (Mitchell and Reigada 2008; Peterson et al. 1997; Tovell and Sanderson 2008). Since ATP-mediated  $\text{Ca}^{2+}$  signaling is broadly involved in RPE physiology, characterizing ATP-induced  $\text{Ca}^{2+}$  responses in RPE monolayers destined for clinical applications is central to the verification of their native-like

functionality (Miyagishima et al. 2016). However, cell-cell variations in response characteristics in RPE monolayer create a challenge and highlight a need for tools to analyze single cell responses from large cell populations. We introduce a method for analyzing ATP-induced  $\text{Ca}^{2+}$  responses from  $\text{Ca}^{2+}$  imaging data over any number of individual cells within a given region of interest (ROI). The analysis allows us to characterize several quantitative response parameters, to use these to find different response groups within the ROI, and to assess homogeneity and quality of the RPE monolayer.

## **XX.2 Materials and Methods**

### ***XX.2.1 Cell culturing and ethical issues***

Human embryonic stem cell (hESC)-derived RPE (08/017) was obtained and characterized as described previously (Korkka et al. 2018; Vaajasaari et al. 2011). Differentiated hESC-RPE cells were cultured on polyethylene terephthalate hanging culture inserts (pore size 1  $\mu\text{m}$ , Merck Millipore) coated with Collagen IV (10  $\mu\text{g}/\text{cm}^2$ , Sigma-Aldrich) and laminin (1.8  $\mu\text{g}/\text{cm}^2$ , LN521TM, Biolamina, Sweden) for 8-13 weeks. The studies were conducted under approval from the National Authority for Medicolegal Affairs, Finland (Dnro 1426/32/300/05), and the Local Ethics Committee of the Pirkanmaa Hospital District, Finland (R05116).

### ***XX.2.2 $\text{Ca}^{2+}$ -imaging***

The cells were loaded with  $\text{Ca}^{2+}$ -sensitive dye fluo-4-acetoxymethyl ester (fluo-4 AM; #F14201, Molecular Probes, Invitrogen) according to the manufacturer's instructions in Elliot solution (pH 7.4, 330 mOsm, containing in mM 137 NaCl, 5 KCl, 0.44  $\text{KH}_2\text{PO}_4$ , 20 HEPES, 4.2  $\text{NaHCO}_3$ , 5 glucose, 1.2  $\text{MgCl}_2$ , and 2  $\text{CaCl}_2$ ). During imaging, hESC-RPE cells were perfused with Elliot solution or Elliot containing 100  $\mu\text{M}$  ATP (Sigma-Aldrich) using a gravity-fed solution exchange

system (ValveBank, AutoMate Scientific). Imaging was performed at room temperature with Nikon Eclipse FN1 microscope using a 25×/1.1 water immersion objective. Fluo-4 images were acquired with standard EGFP imaging settings every 500 ms for 10 min per single time lapse. Baseline imaging was performed for 2 min after which the cells were exposed to 100 μM ATP for 2 min followed by imaging for additional 6 min in Elliot.

### ***XX.2.3 Data analysis***

The intensity data from the fluorescence images were obtained with ImageJ (version 1.52e). Three 200x200 pixel ROIs were cropped from each Ca<sup>2+</sup> image stacks (n=18). The stacks were segmented by roughly outlining cells as circles from the images (diameter ~10 μm). All cells recognizable with reasonable certainty were outlined, resulting in approximately 70–120 cells per ROI. The intensity data from all segments, as well as the average intensity over the ROI were extracted to a spreadsheet as a function of time.

The analysis of the intensity data was developed in MATLAB (R2017b). The data was read into MATLAB to have each cell appear as an object with its own time and intensity data. Scripts were written to correct for photobleaching, filtering out noise and to calculate the response parameters. All the calculated data were added as parameters to the cell objects. The clustering of the Ca<sup>2+</sup>-response curves based on the parameters was performed using built-in principal component analysis and hierarchical clustering functions in MATLAB.

## **XX.3 Results**

### **Imaging of ATP-induced Ca<sup>2+</sup> -responses in RPE monolayer**

ATP-induced Ca<sup>2+</sup> responses were measured from intact, pigmented and polarized hESC-RPE monolayers with typical cobblestone morphology (Fig. XX.1a). To visualize the recorded Ca<sup>2+</sup>

response, grayscale images of Fluo-4 loaded cells are shown as pseudocolored images (Fig. XX.1b). Applying 100  $\mu\text{M}$  ATP in perfusate for 2 min induced a strong  $\text{Ca}^{2+}$  response in the whole epithelium (Fig. XX.1c). This response was further analyzed both from the whole field fluorescence data and at the level of single cells (Fig. XX.1d, highlighted cells in Fig. XX.1b&c). The single cell data indicated that measuring only the average response from the whole image does not necessarily represent the behavior of individual cells in the field. In our example (Fig. XX.1d), Cells 1 and 2 possess distinctively different response characteristics: Cell 1 had a slower initial increase of the response (release from intracellular stores) compared to Cell 2, together with smaller amplitude and a slower secondary response (extracellular  $\text{Ca}^{2+}$  influx). This indicates considerable heterogeneity even among cells that are not physically far from each other.

### **Detailed analysis of response characteristics**

Five quantitative parameters were calculated from the intensity response data (Fig. XX.2a): 1) Maximum amplitude ( $A_{max}$ ) describing the maximum relative intensity change (normalized to the baseline intensity), 2) Rise time ( $T_{rise}$ ) to 50% of the  $A_{max}$ , 3) Time to maximum ( $T_{max}$ ) from the start of the response to the  $A_{max}$ , 4) Decay time ( $T_{dec}$ ) from the  $A_{max}$  to 50% intensity, and 5) Response duration ( $T_{dur}$ ) as peak width at half maximum. These parameters characterize the basic shape of the response. When this analysis was conducted to Cell 1 and Cell 2 from Fig. XX.1, their  $A_{max}$  and  $T_{rise}$  parameters indicated clearly different response kinetics (Fig. XX.2b).

### **Analysis of response characteristics from cell population**

The determined response parameters can be used to characterize the whole cell population at the single cell level. This allows further analysis of correlations between parameters and grouping of

cells to different response types. The process was automated by using MATLAB (see Supplementary information for details).

As an example of whole population single cell analysis, we quantified the  $\text{Ca}^{2+}$ -response from 87 cells from a single image field and analyzed their response kinetics (Fig. XX.3). We visualized the different parameters by using scatter plots. The plots indicated positive correlation between  $T_{dec}$  and  $T_{dur}$ , whereas correlation between  $T_{rise}$  and  $T_{dur}$  appeared negative. Interestingly  $T_{dur}$  and  $A_{max}$  did not correlate. Cells 1 and 2 from the previous figures are marked in each scatter plot, revealing their different nature among the cell population.

We grouped the  $\text{Ca}^{2+}$  responses according to the analyzed parameters. The grouping algorithm was optimized to find two to four clusters from the data that differ by their response characteristics. In the case of our example image field, the algorithm found three clusters with 11-46 responses in each, and their responses are shown in Fig. XX.3b. The black curves highlight responses whose parameters describe the group averages the best. The groups are visualized in the scatter plots with respective colors, showing their location in the parameter space. This population data brings out the major differences in response types between the groups. Our example Cells 1 and 2 belong to groups 3 and 1, respectively.

#### **XX.4 Discussion**

Changes in  $[\text{Ca}^{2+}]_i$  have a critical impact on the functioning of RPE (Wimmers et al. 2007). Measuring  $\text{Ca}^{2+}$  dynamics in RPE by  $\text{Ca}^{2+}$  imaging or patch clamp is thus important for addressing its physiology and stem cell-derived RPE differentiation, maturation and authenticity (Korkka et al. 2018; Miyagishima et al. 2016; Reichhart and Strauss 2014; Singh et al. 2013). Here, we developed tools to analyze  $\text{Ca}^{2+}$  imaging data from RPE monolayers at single cell level. Our focus was in ATP-induced  $\text{Ca}^{2+}$  response characteristics that reflect  $\text{Ca}^{2+}$  signaling pathways including

Ca<sup>2+</sup> release from intracellular stores and membrane conductances (Reichhart and Strauss 2014). When analyzing Ca<sup>2+</sup> responses from large fields of polarized hESC-RPE monolayers, we observed significant cell-cell variation. Earlier work on induced pluripotent stem cell-derived RPE has indicated variations in Ca<sup>2+</sup> responses between preparations (Miyagishima et al. 2016). Moreover, single cell and population level analysis of Ca<sup>2+</sup> dynamics in lens capsule epithelium has revealed cell-cell variability comparable to our study (Gosak et al. 2015). With the analysis tools developed in this work, we could parametrize the heterogeneity of the measured responses. This allowed us to further group the cells according to their response characteristics and to assess population data from hESC-RPE monolayers across different samples. Following response kinetics can be biologically highly significant since the initial rising phase of the ATP-induced response results from the release of Ca<sup>2+</sup> from intracellular stores via P2Y<sub>2</sub> receptors and the secondary response from extracellular Ca<sup>2+</sup> influx (Tovell and Sanderson 2008). Detailed analysis has the potential to advance identification of Ca<sup>2+</sup> signaling pathways contributing to RPE functions and to help in authentication of stem cell-derived RPE.

## **Acknowledgments**

The authors thank Dr. Heli Skottman for cell lines, Julia Johansson, Viivi Jokinen, Outi Heikkilä and Outi Melin for technical assistance. The study was supported by Academy of Finland (grants 287287, 267471) and Emil Aaltonen Foundation.

## **References**

Gosak M, Markovič R, Fajmut A et al (2015) The Analysis of Intracellular and Intercellular Calcium Signaling in Human Anterior Lens Capsule Epithelial Cells with Regard to Different Types and Stages of the Cataract. PLoS One 4;10:e0143781

- Korkka I, Viheriälä T, Juuti-Uusitalo K et al (2018) Functional Voltage-Gated Calcium Channels Are Present in Human Embryonic Stem Cell-Derived Retinal Pigment Epithelium. *Stem Cell Transl Med, In Press*
- Mitchell CH, Reigada D (2008) Purinergic signalling in the subretinal space: a role in the communication between the retina and the RPE. *Purinergic Signal* 4:101-107
- Miyagishima KJ, Wan Q, Corneo B et al (2016) In Pursuit of Authenticity: Induced Pluripotent Stem Cell-Derived Retinal Pigment Epithelium for Clinical Applications. *Stem Cells Transl Med* 5:1562–1574
- Peterson WM, Meggyesy C, Yu K et al (1997) Extracellular ATP activates calcium signaling, ion, and fluid transport in retinal pigment epithelium. *J Neurosci* 17:2324–2337
- Reichhart N, Strauss O 2014 Ion channels and transporters of the retinal pigment epithelium. *Exp Eye Res* 126:27-37
- Singh R, Phillips MJ, Kuai D et al (2013) Functional analysis of serially expanded human iPS cell-derived RPE cultures. *Invest Ophthalmol Vis Sci.* 17;54:6767-6778
- Strauss O (2005) The retinal pigment epithelium in visual function. *Physiol Rev* 85:845–881
- Tovell VE, Sanderson J (2008) Distinct P2Y receptor subtypes regulate calcium signaling in human retinal pigment epithelial cells. *Invest Ophthalmol Vis Sci* 49:350-357
- Vaajasaari H, Ilmarinen T, Juuti-Uusitalo K et al (2011) Toward the defined and xeno-free differentiation of functional human pluripotent stem cell-derived retinal pigment epithelial cells. *Mol Vis* 22:558-575
- Wimmers S, Karl MO, Strauss O (2007) Ion channels in the RPE. *Prog Retin Eye Res.* 2007 26:263-301



## Figures

### Fig XX.1 ATP-induced $\text{Ca}^{2+}$ response in RPE monolayer

**a:** Brightfield image of mature RPE monolayer **b:** Gray scale (left) and pseudocolored (right) images of Fluo-4  $\text{Ca}^{2+}$ -indicator in RPE, with two individual cells highlighted. **c:** Pseudocolored time series during a typical ATP-induced  $\text{Ca}^{2+}$  response. **d:** Relative intensity of Cell 1, Cell 2, and the ROI average plotted against time. Scale bars  $20\mu\text{m}$ .

### Fig XX.2 Analysis of $\text{Ca}^{2+}$ response kinetics

**a:** Schematic  $\text{Ca}^{2+}$  response curve presenting the parameters calculated from the data ( $A_{max}$  = maximum relative amplitude,  $T_{rise}$  = rise time to 50% of  $A_{max}$ ,  $T_{max}$  = time to  $A_{max}$ ,  $T_{dec}$  = decay time from  $A_{max}$  to 50% of  $A_{max}$ ,  $T_{dur}$  = response duration above 50% of  $A_{max}$ ) **b:** Responses of Cell 1 and 2 from Fig. XX.1 showing  $A_{max}$  and  $T_{rise}$  with values in the table.

### Fig XX.3 $\text{Ca}^{2+}$ response characteristics and grouping

**a:** Scatter plots of  $T_{dur}$  and  $A_{max}$  (left),  $T_{dec}$  (middle) or  $T_{rise}$  (right) revealing no-correlation, positive correlation and negative correlation between the parameters, respectively. The locations of Cell 1 and 2 are highlighted. **b:** Three  $\text{Ca}^{2+}$  response groups obtained by a hierarchical clustering algorithm using the parameters from Fig XX.2. The black line represents the response closest to the group average values.

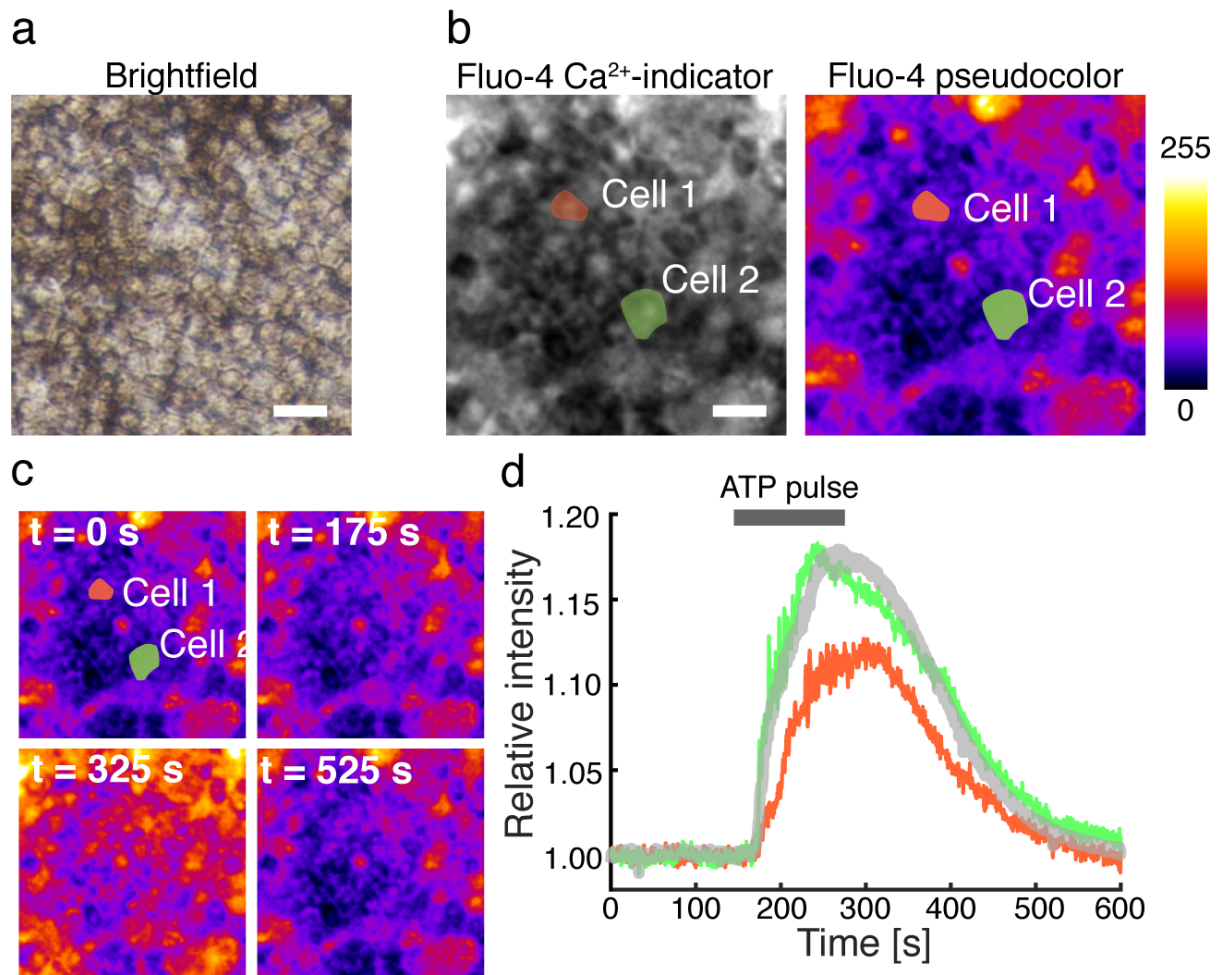


Figure 1

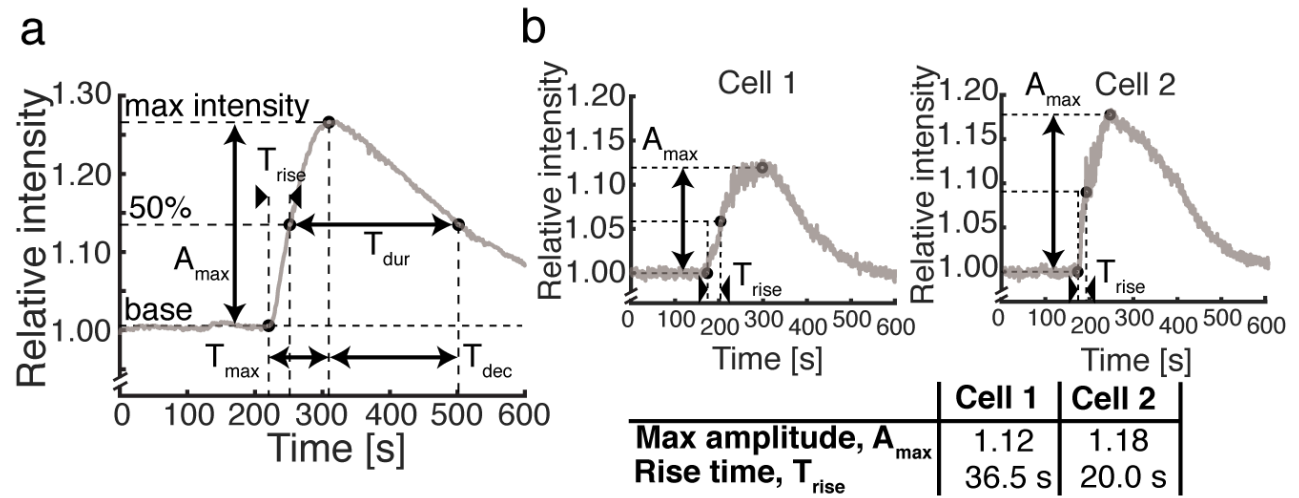


Figure 2

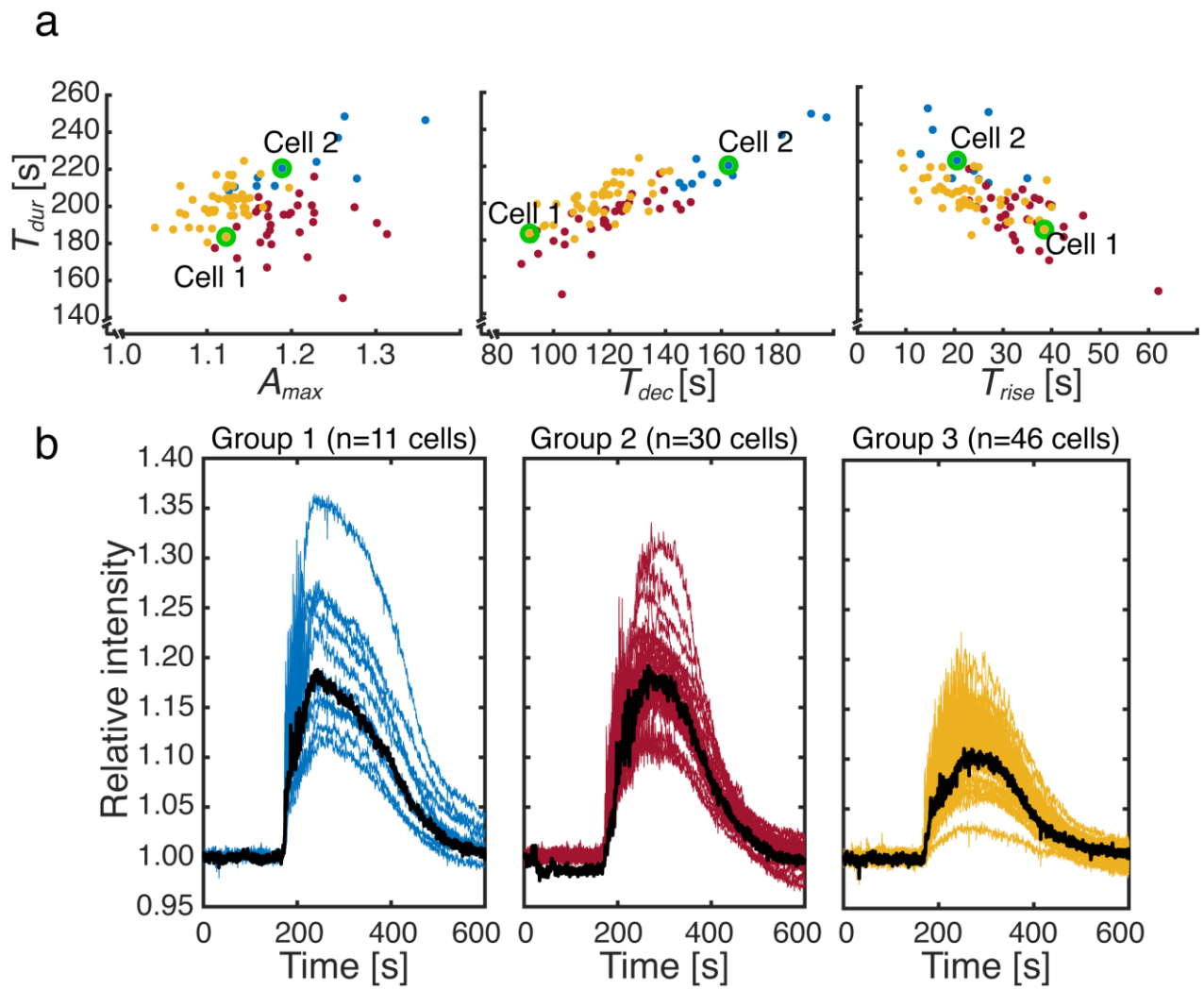


Figure 3